IRIS BIOMETRIC SYSTEM

CS635

Dept. of Computer Science & Engineering
NIT Rourkela

Iris Biometrics

- Iris is externally-visible, colored ring around the pupil
- The flowery pattern is unique for each individual
- The right and left eye of any given individual, have unrelated iris patterns
- Iris is stable throughout life
- Randomness

Anatomical Structure of Iris

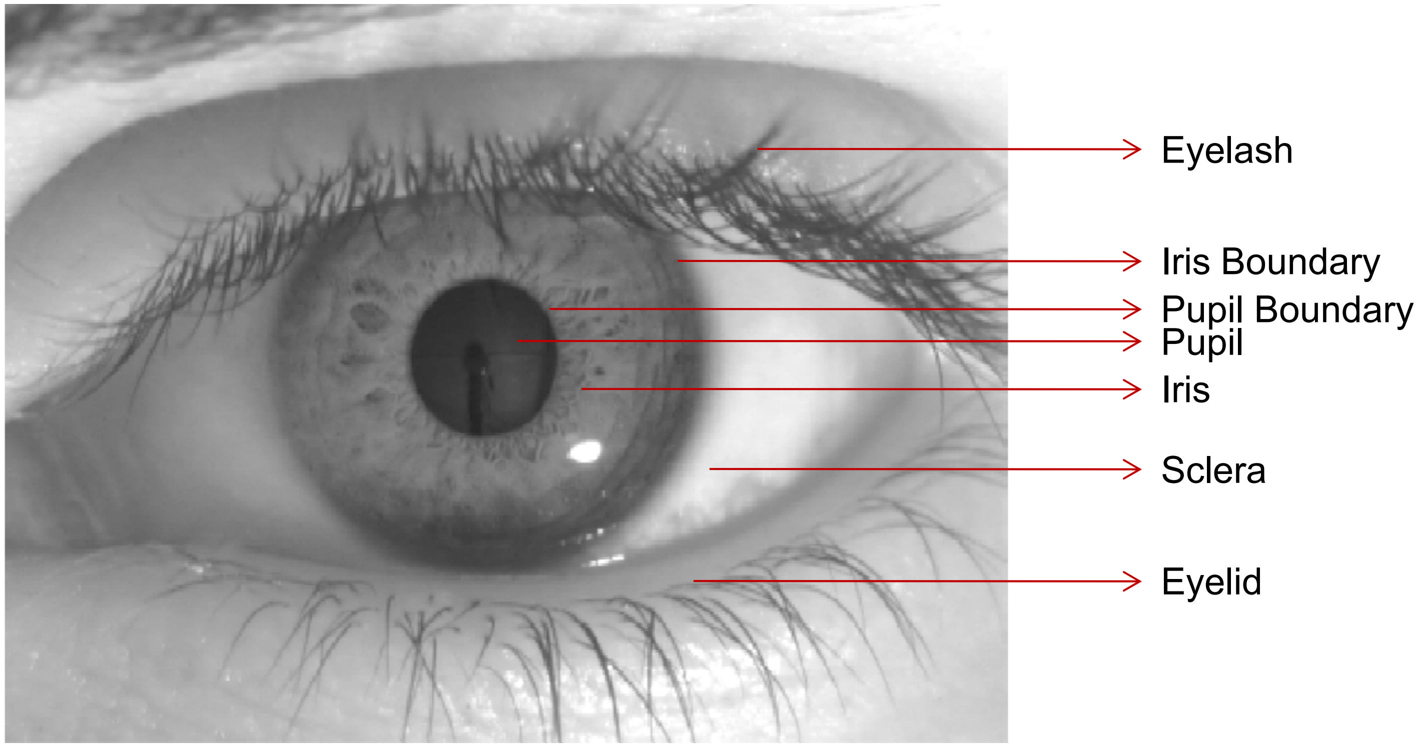

Advantages of Iris Recognition

- Highly protected, internal organ of the eye
- Externally visible patterns imaged from a distance
- Patterns apparently stable throughout life
- Iris shape is far more predictable than that of the face
- No need for a person to touch any equipment

Disadvantages of Iris Recognition

- Localization fails for dark iris
- Highly susceptible for changes in weather or due to infection
- Obscured by eyelashes, lenses, reflections
- Well trained and co-operative user is required
- Expensive Acquisition Devices

Occlusion due to eyelashes

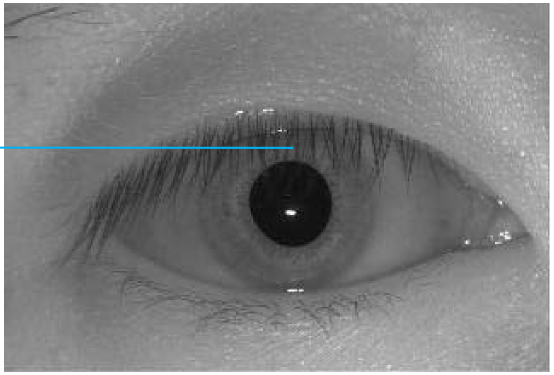

The remarkable story of Sharbat Gula, first photographed in 1984 aged 12 in a refugee camp in Pakistan by National Geographic photographer Steve McCurry, and traced 18 years later to a remote part of Afghanistan where she was again photographed by McCurry, is told by National Geographic in their magazine (April 2002 issue)

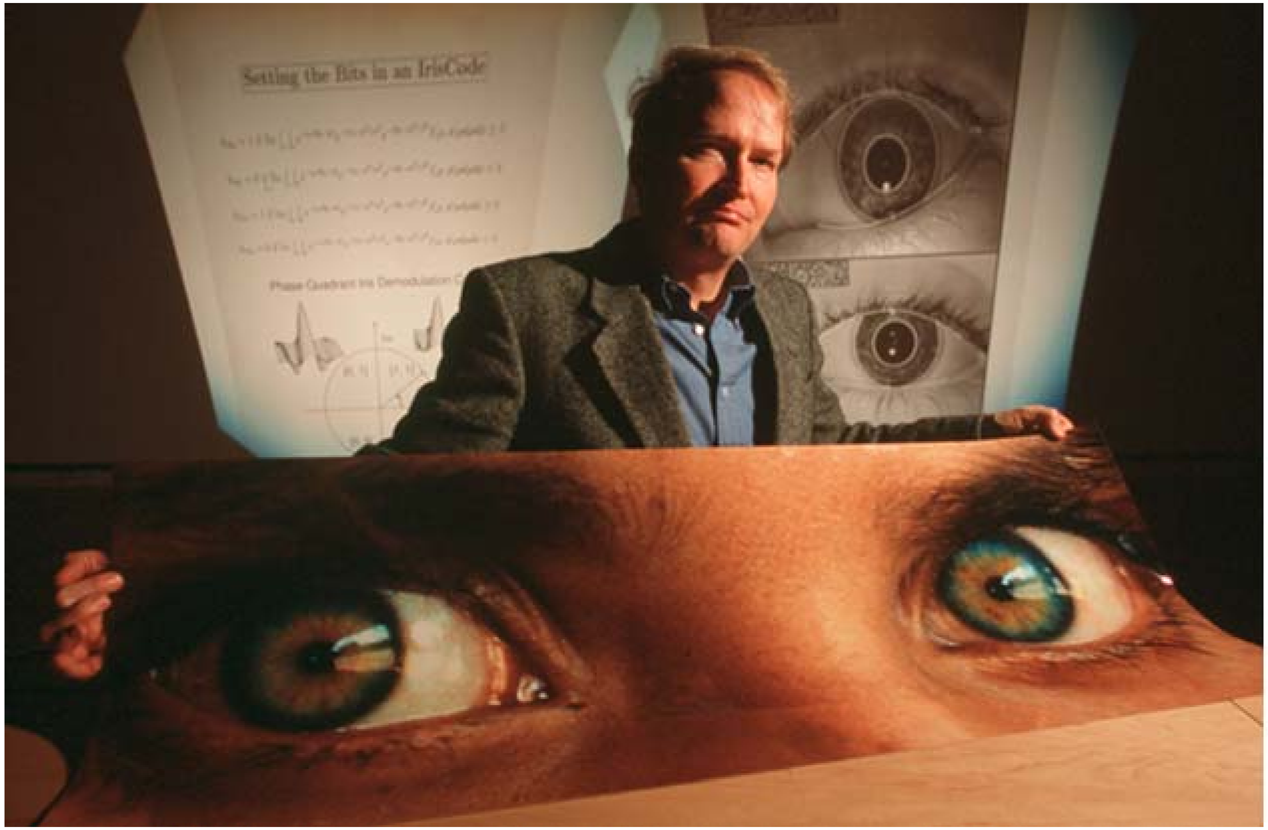

Photograph by Alexandra Boulat

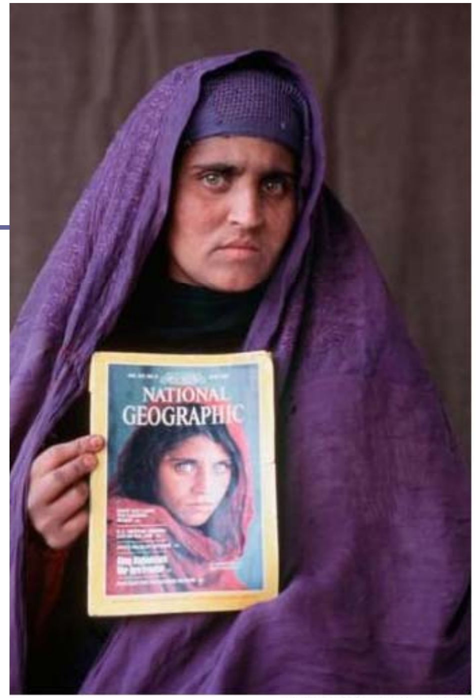

Photograph by Steve McCurry

Geographic turned to the inventor of automatic iris recognition, John Daugman, a professor of computer science at England's University of Cambridge. His biometric technique uses mathematical calculations, and the numbers Daugman got left no question in his mind that the haunted eyes of the young Afghan refugee and the eyes of the adult Sharbat Gula belong to the same person.

Generic Iris Biometric System

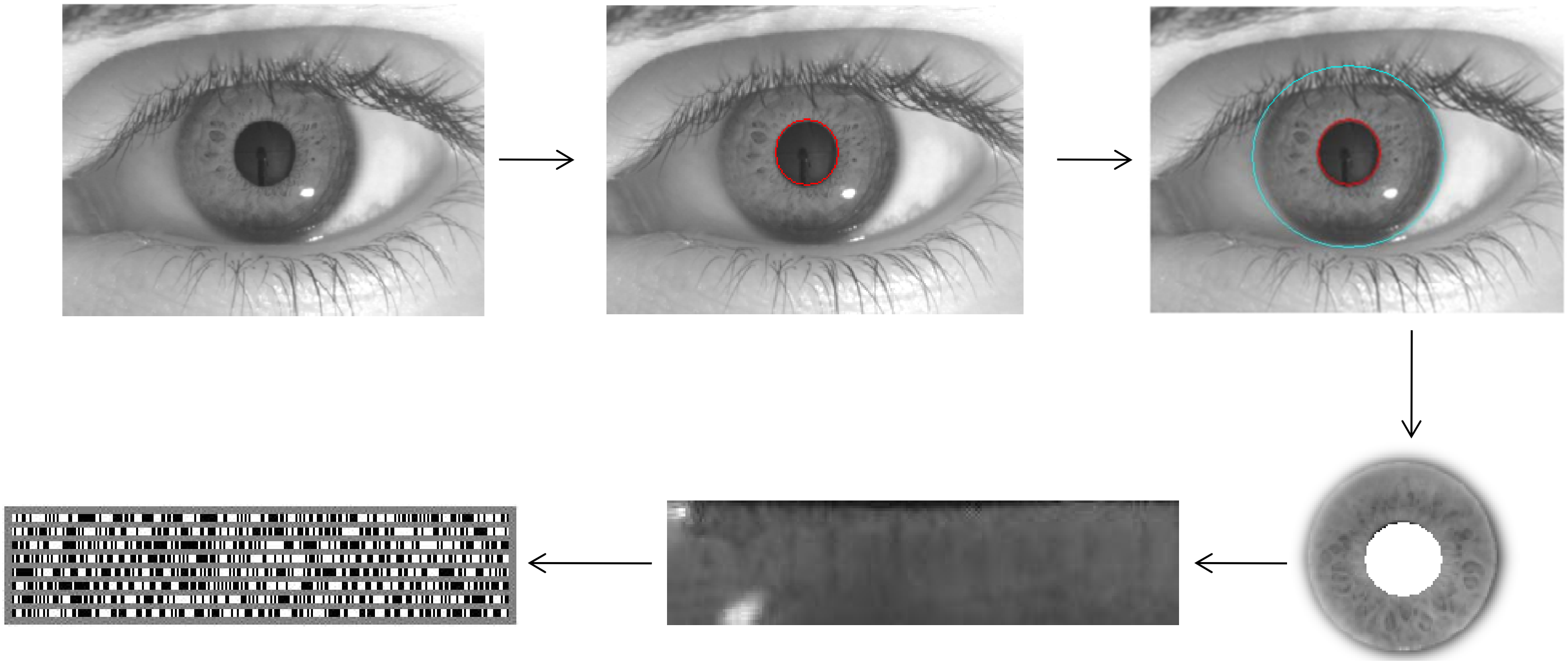

Literature Review

- Flom and Safir
- Daugman’s Approach
- Wildes Approach
- Proposed Implementation

Flom and Safir

- In 1987 the authors obtained a patent for an unimplemented conceptual design of an iris biometrics system

- Their description suggested
  - highly controlled conditions
  - headrest
  - target image to direct the subject's gaze
  - manual operator
  - Pupil expansion and contraction was controlled by changing the illumination to force the pupil to a predetermined size

- To detect the pupil,
  - Threshold based approach

- Extraction of Iris Descriptors
  - Pattern recognition tools
  - Edge detection algorithms
  - Hough transform

- Iris features could be stored on a credit card or identification card to support a verification task

Daugman’s Approach

- Daugman’s 1994 patent described an operational iris recognition system in some detail.
- Improvements over Flom and safir’s approach
- Image Acquisition
  - Image should use near-infrared illumination
- Iris Localization
  - An integro-differential operator for detecting the iris boundary by searching the parameter space.
- Iris Normalization
  - mapping the extracted iris region into polar coordinate system

- Feature Encoding
  - 2D Wavelet demodulation

- Matching
  - Hamming distance, which measures the fraction of bits for which two iris codes disagree

Wildes Approach

- Wildes describes an iris biometrics system developed at Sarnoff Labs
- Image Acquisition
  - a diffuse light source
  - low light level camera
- Iris Localization
  - Computing an binary edge map
  - Hough transform to detect circles
- Feature Extraction
  - Laplacian of Gaussian filter at multiple scales
- Matching
  - normalized correlation

Proposed Implementation

- The iris recognition system developed consists of
  - Image Acquisition
  - Preprocessing
  - Iris Localization
    - Pupil Detection
    - Iris Detection
  - Iris Normalization
  - Feature Extraction
    - Haar Wavelet
  - Matching

Image Acquisition

- The iris image is acquired from a CCD based iris camera
- Camera is placed 9 cm away from subjects eye
- The source of light is placed at a distance of 12 cm (approx) from the user eye
- The distance between source of light and CCD camera is found to be approximately 8 cm

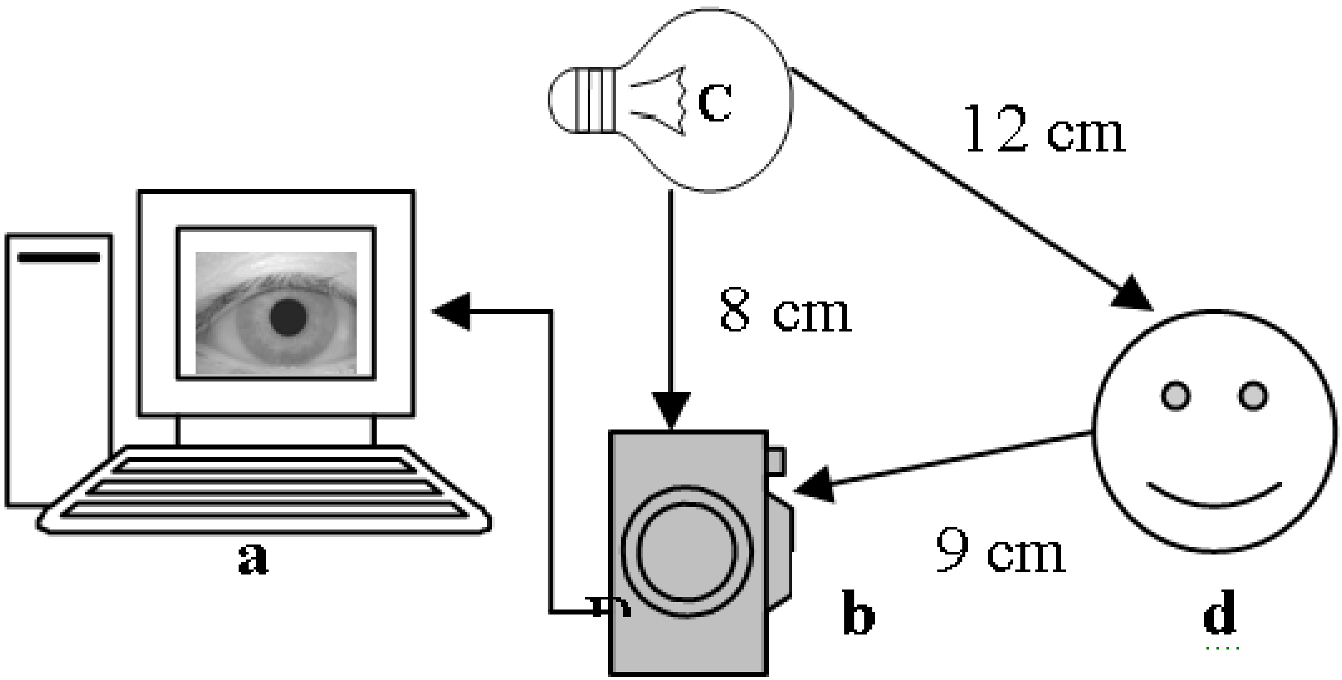

Image Acquisition System: (a) System with frame grabber
(b) CCD Camera (c) Light Source (d) User

Preprocessing

- The detection of pupil fails whenever there is a spot on the pupil area
- Preprocessing removes the effect of spots/holes lying on the pupillary area.
- The preprocessing module first transforms the true color (RGB) into intensity image

Steps involved in preprocessing

- Binarization
- Find the complement of binary image
- Hole filling using four connected approach
- Complement of hole filled image

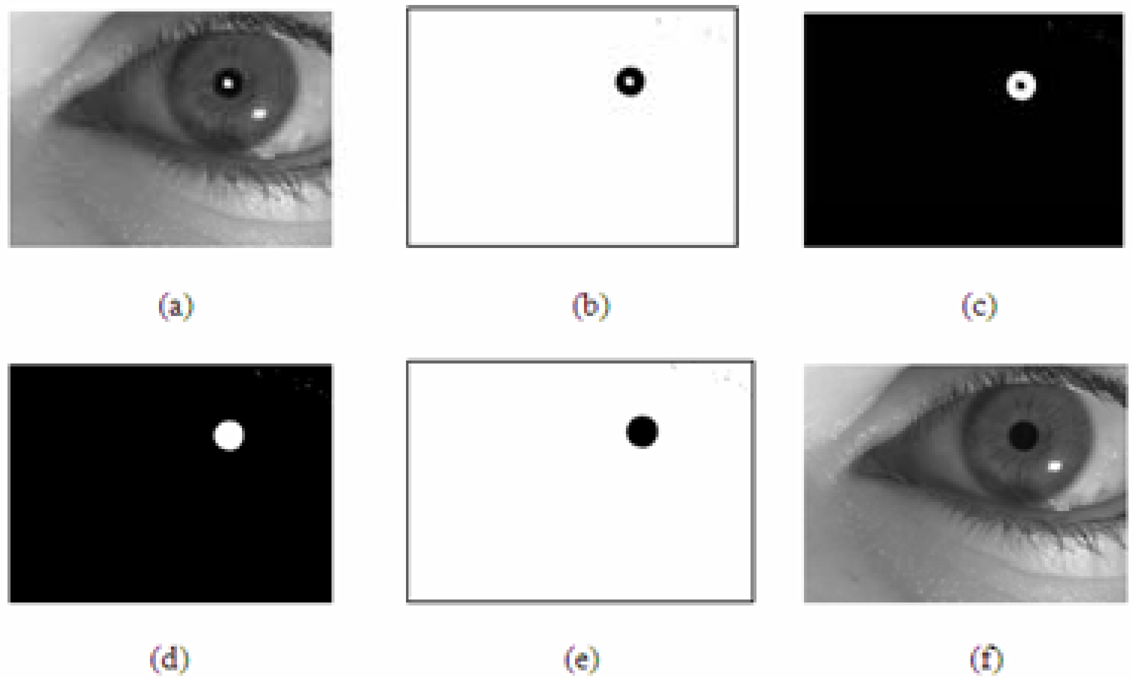

Preprocessing and noise removal

Iris Localization

- The important steps involved in iris localization are
  - Pupil Detection
  - Iris Detection

Pupil Detection

- The steps involved in pupil detection are
  - Thresholding
  - Edge Detection
  - Circular Hough Transform

Thresholding

- Pupil is the darkest portion of the eye
- The pupil area is obtained after thresholding the input image

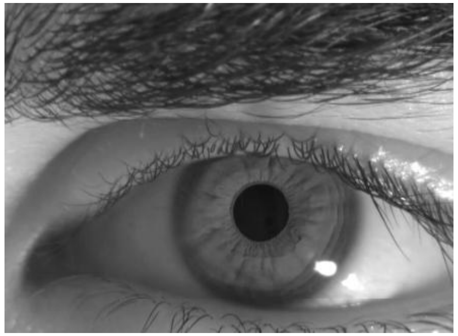

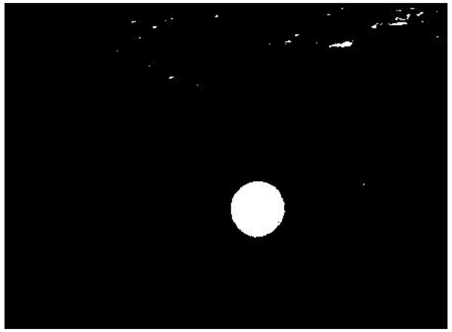

Edge Detection

- After thresholding the image edge is obtained using *Canny edge Detector*

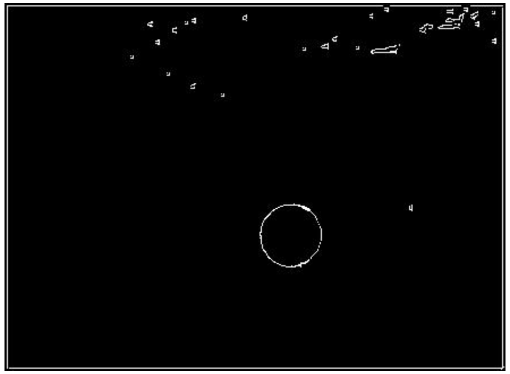

Circular Hough Transform (CHT)

- CHT is used to transform a set of edge points in the image space into a set of accumulated votes in a parameter space

- For each edge point, votes are accumulated in an accumulator array for all parameter combinations.

- The array elements that contain the highest number of votes indicate the presence of the shape

- For every edge pixel (p) find the candidate center point using

$$x_t = x_p - r \times \cos(\theta)$$

$$y_t = y_p - r \times \sin(\theta)$$

where x_p and y_p is the location of edge point p

r ϵ [r_{min} r_{max}]

x_t and y_t is the determined circle center

- For range of radius
  - The center point is computed
  - The Accumulator array is incremented by one for calculated center point
  - $Accum[x_t,y_t,r]=Accum[x_t,y_t,r]+1$

- The point with maximum value in the accumulator is denoted as circle center with radius r

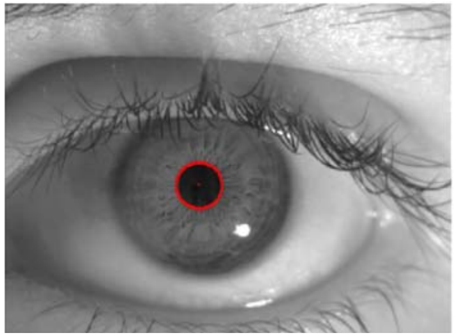

Iris Detection

- Steps involved are
  - Histogram Equalization
  - Concentric Circles of different radii are drawn from the detected pupil center
  - The intensities lying over the perimeter of the circle are summed up
  - Among the candidate iris circles, the one having a maximum change in intensity with respect to the previous drawn circle is the iris outer boundary

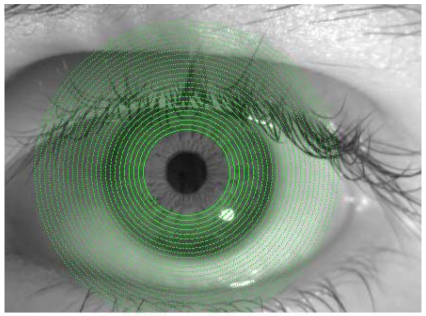

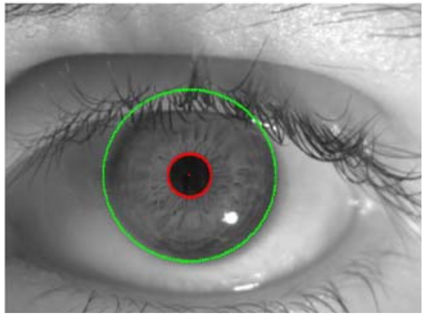

(a) Histogram Equalization (b) Concentric Circles (c) Iris Detected

Iris Normalization

- Localizing iris from an image delineates the annular portion from the rest of the image

- The annular ring is transformed to rectangular ring

- The coordinate system is changed by unwrapping the iris from Cartesian coordinate their polar equivalent

$$
\begin{aligned}
& I(x(\rho,\theta), y(\rho,\theta)) \rightarrow I(\rho,\theta) \\
& with \\
& x_p(\rho,\theta) = x_{\rho 0}(\theta) + r_p * \cos(\theta) \\
& y_p(\rho,\theta) = y_{\rho 0}(\theta) + r_p * \sin(\theta) \\
& x_i(\rho,\theta) = x_{i0}(\theta) + r_i * \cos(\theta) \\
& y_i(\rho,\theta) = x_{i0}(\theta) + r_i * \sin(\theta)
\end{aligned}
$$

- where *rp* and *ri* are respectively the radius of pupil and the iris
- while *(xp(θ), yp(θ))* and *(xi(θ), yi(θ))* are the coordinates of the pupillary and limbic boundaries in the direction *θ*. The value of *θ* belongs to [0;2π], ρ belongs to [0;1]

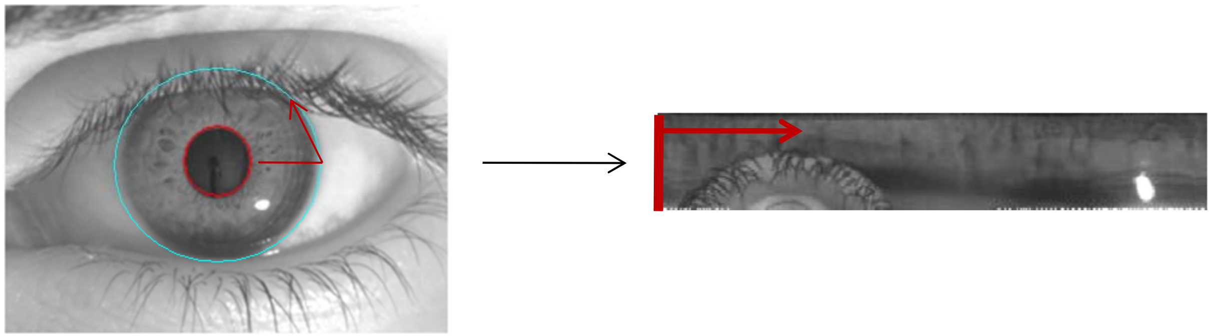

Recognition using Haar Wavelet

- One dimensional transformation on each row followed by one dimensional transformation of each column.

- Extracted coefficients would be
  - Approximation
  - Vertical
  - Horizontal
  - Diagonal

- Approximation coefficients are further decomposed into the next level

- 4 level decomposition is used

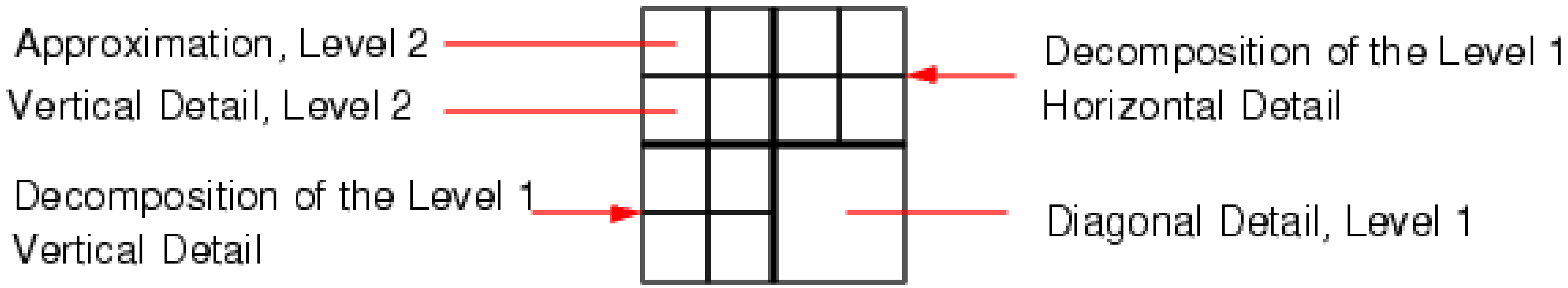

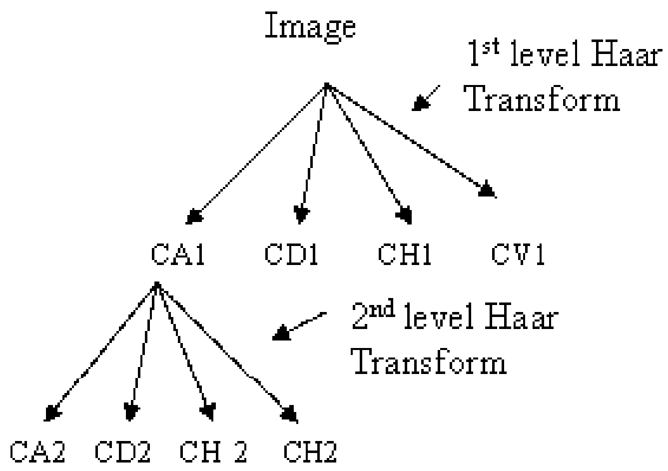

Graphical Representation - Wavelet decomposition
(level = 2)

Approach

- For a 2X2 matrix

$$x = \overrightarrow{\begin{pmatrix} a & b \\ c & d \end{pmatrix}} \qquad x = \begin{pmatrix} a+b & a-b \\ c+d & c-d \end{pmatrix}\Big\downarrow$$

$$y = \frac{1}{2}\begin{pmatrix} a+b+c+d & a-b+c-d \\ a+b-c+d & a-b-c+d \end{pmatrix}$$

Example

2	2	9	5
2	0	5	2
6	7	4	7
3	4	8	8

Column wise Summation

4	14	0	4
2	7	2	3
13	11	-1	-3
7	16	-1	0

Row wise Summation

6	21	2	7
20	27	-2	-3
2	7	-2	1
6	-5	0	-3

Finding Average

Approximation Horizontal

3	10.5	1	3.5
10	13.5	-1	-1.5
1	3.5	-1	0.5
3	-2.5	0	-1.5

Vertical Diagonal

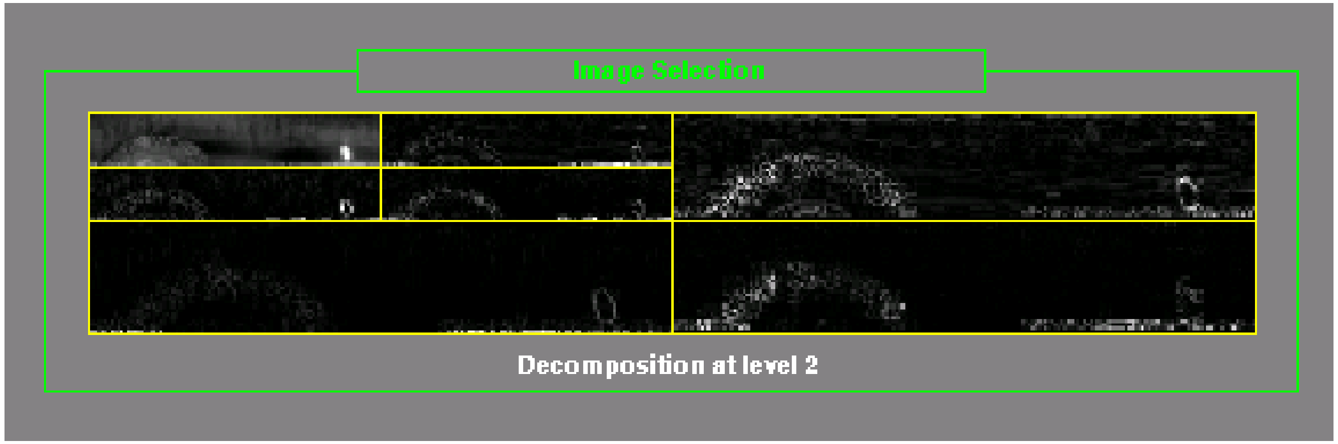

Iris Strip after Decomposition

Feature Template

- At level 4 coefficient matrices are combined into single feature matrix or feature template FV= [CD_4 CV_4 CH_4].

$$Iris(i) = \begin{cases} 1 & FV(i) \geq 0 \\ 0 & FV(i) < 0 \end{cases}$$

where Iris is the binarized iris code

Matching

- Database template (S) is matched with the query template (T) using Hamming distance approach

$$MS_{Iris} = \frac{1}{n \times m} \sum_{\substack{i=1 \\ j=1}}^{\substack{n \\ m}} T_{i,j} \otimes S_{i,j}$$

where n X m is the size of template and $\otimes$ is the bitwise xor

Institutes working - Databases

Bath University

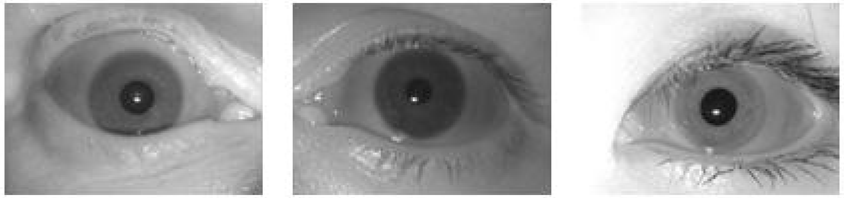

MMU

UBIRIS

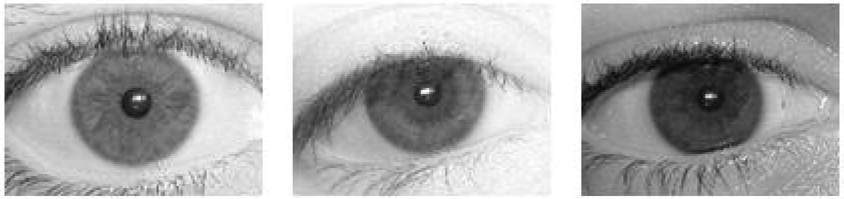

Casia V3

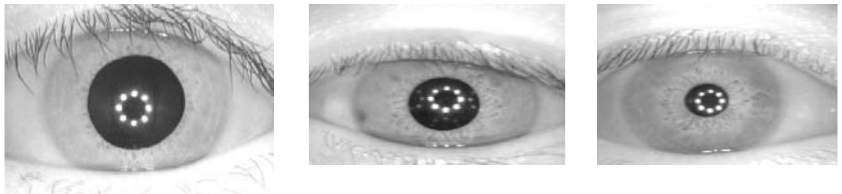

IIT Kanpur

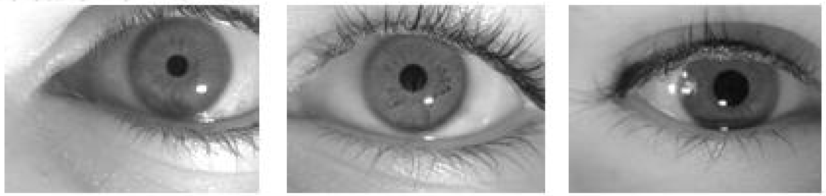

Databases Used

Name	Images (Subject × Images per subject = Total Images)
BATH	50 × 20 = 1000
CASIA V3	249 × 11 ≈ 2655 (approx)
Iris IITK	600 × 3 = 1800

Performance

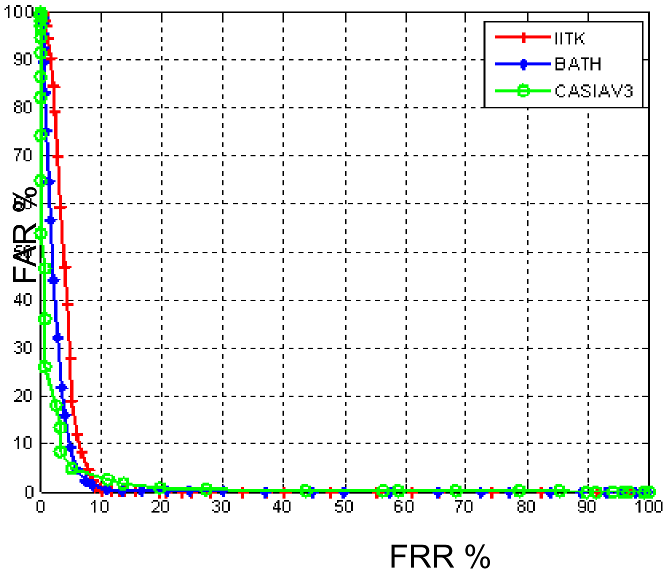

Database	Accuracy (%)	FAR (%)	FRR (%)
IIT Kanpur	94.87	1.06	9.18
Bath University	95.08	2.33	7.50
CASIAV3	95.07	4.71	5.12

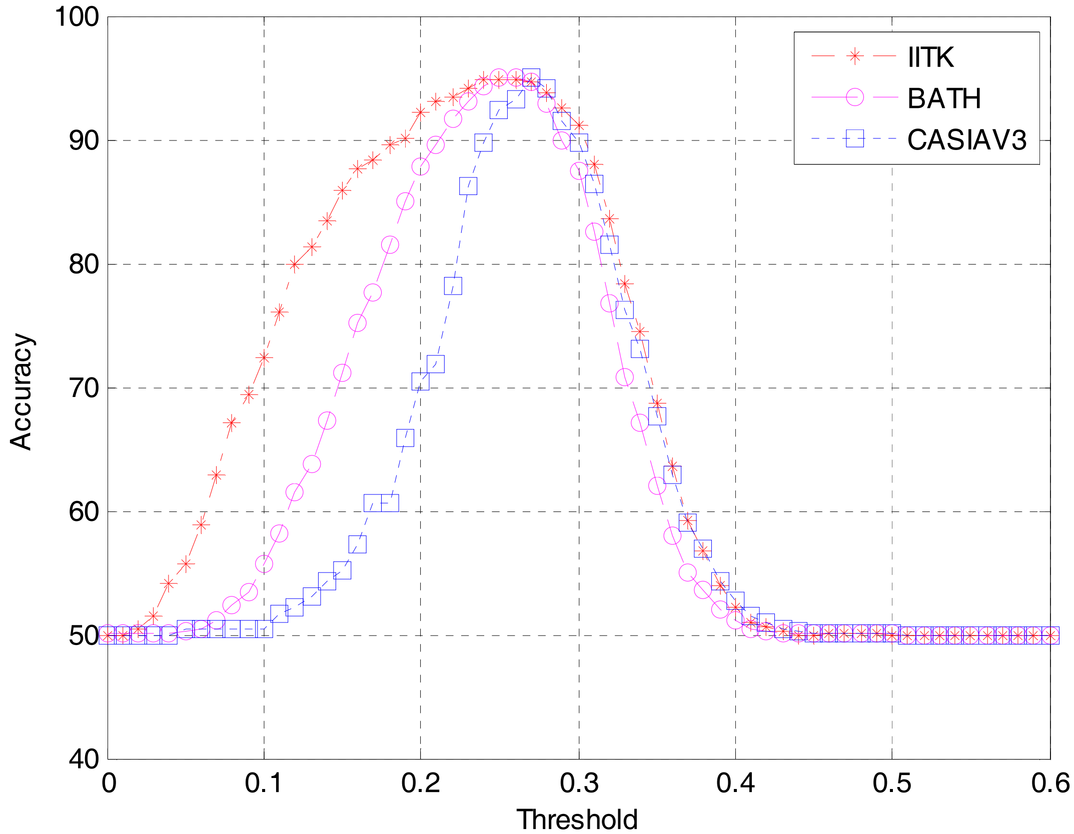

Accuracy Graph vs. Threshold Graph

Some more work on Iris..

- Matching score level fusion
- Dual stage approach for Iris feature extraction
- Feature level clustering of large biometric database
- Indexing database using energy histogram
- Local feature descriptor for Iris
- Use of annular iris images for recognition

Matching Score Level Fusion

- A novel technique for iris using texture and phase features

- Texture features
  - Haar Wavelet

- Phase features
  - LOG Gabor Wavelet

- Fusion
  - Weighted Sum of Score technique

$$MS_{final} = \alpha \times MS_{Haar} + \beta \times MS_{Gabor}$$

where α and β are static value of weights

Results

Table Showing accuracy values in percentage for BATH and CASIA database

Databases →	**BATH**			**IITK**		
Approaches ↓	FAR	FRR	Acc	FAR	FRR	Acc
Haar Wavelet	1.61	11.08	93.64	0.33	7.88	95.89
LOG Gabor	1.63	9.55	94.40	1.30	6.05	96.31
Fusion	0.36	8.38	95.62	0.16	4.50	97.66

Accuracy Graphs

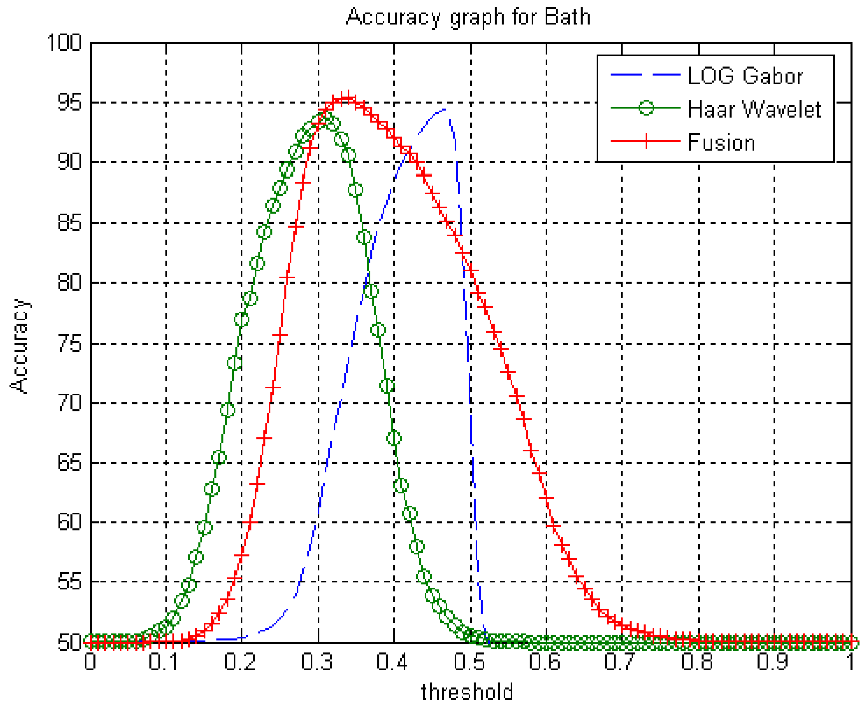

(a) BATH

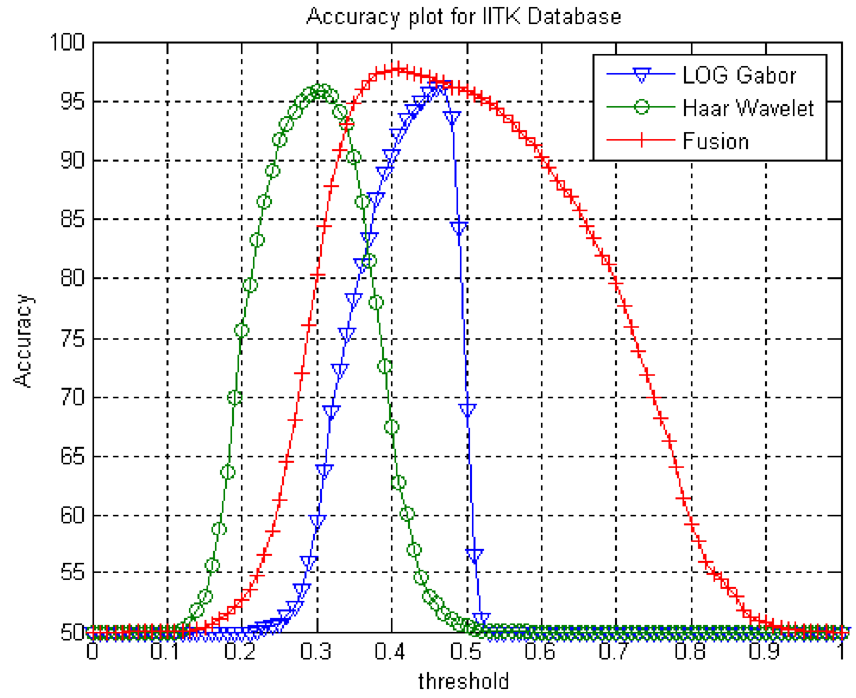

(b) IITK

ROC Curves

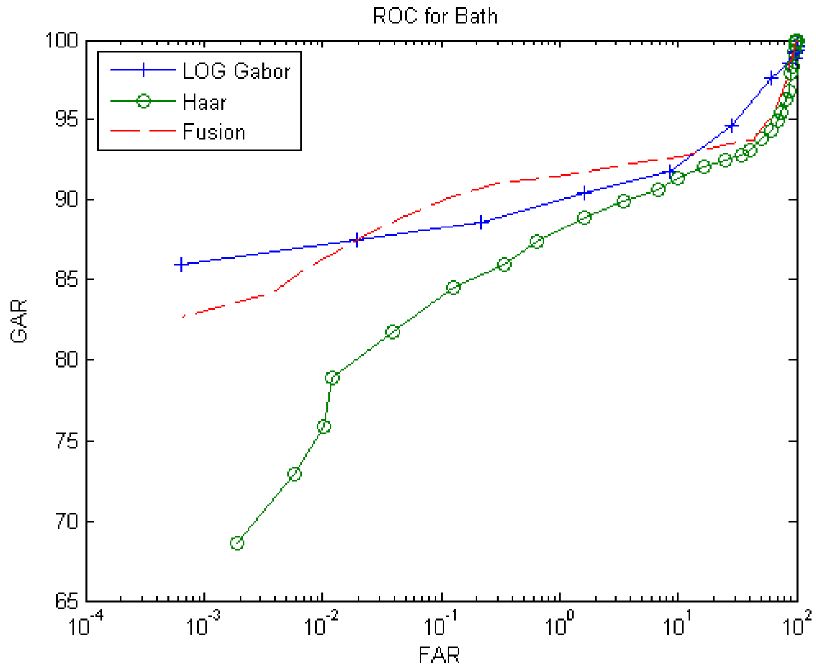

(a) BATH

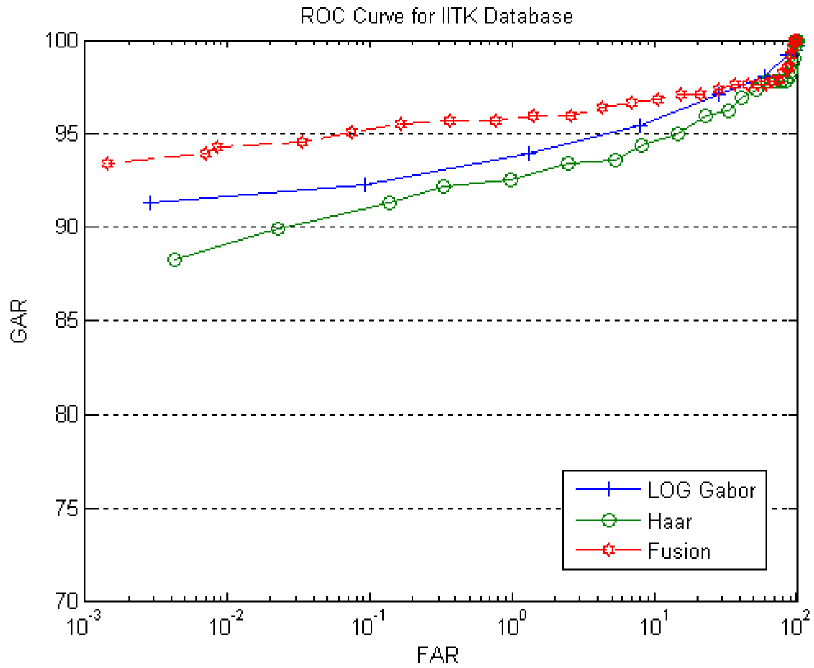

(b) IITK

Dual Stage Approach for IRIS Feature Extraction

- Features are detected
  - Harris Corner Detector
    - Autocorrelation matrix

- For each detected corner (*i*), following information is recorded
  - (x, y)
    - coordinates of i^{th} corner point
  - H_i
    - entropy information of window (w_i) around the corner

- Matching is done in dual stage
  - Stage 1: Pairing corner points using Euclidean distance
  - Stage 2: Finding Mutual Information (MI) of potential corners

Results

TABLE I
FAR, FRR AND ACCURACY VALUES FOR INDIVIDUAL AND COMBINED CLASSIFIERS USING BATH, CASIA AND IITK DATASETS

Datasets	Euclidean Distance			MI			Dual Stage		
	FAR (%)	FRR (%)	Accuracy (%)	FAR (%)	FRR (%)	Accuracy (%)	FAR (%)	FRR (%)	Accuracy (%)
BATH	29.04	39.03	65.97	22.61	31.61	72.89	14.91	10.25	87.42
CASIA	17.18	34.73	74.05	14.91	10.89	87.09	02.64	11.80	92.78
IITK	24.95	21.95	76.55	08.65	22.43	84.46	02.61	00.00	98.70

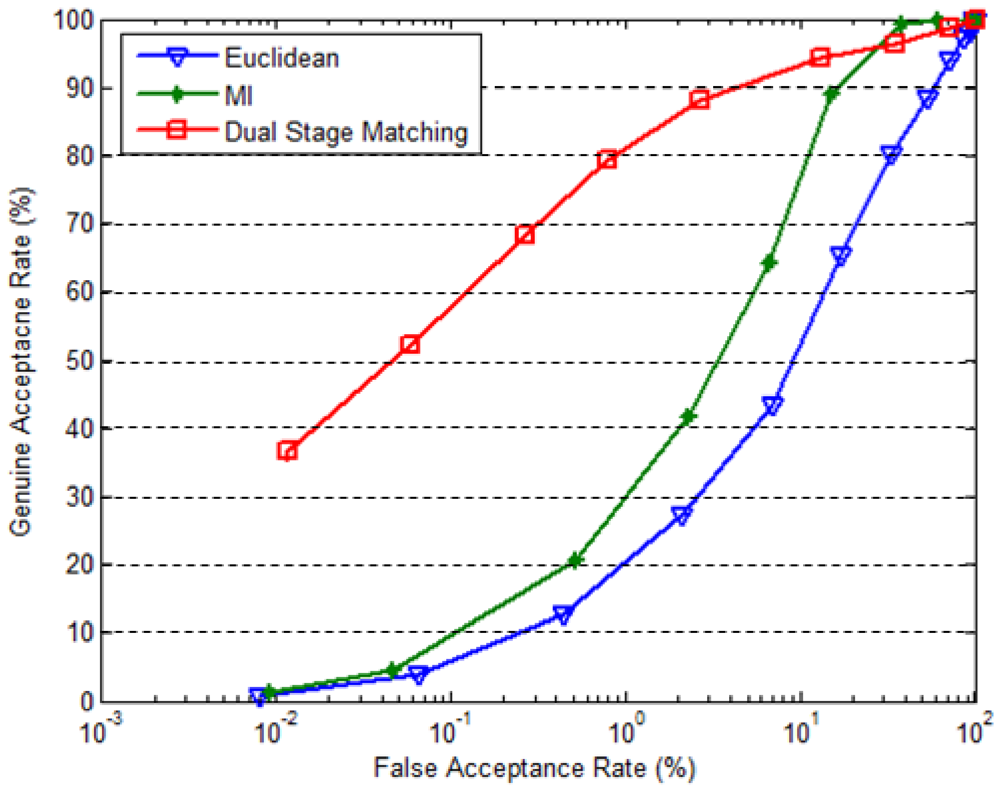

ROC Curve for Euclidean, MI and Dual Stage approach on CASIA Dataset

Feature Level Clustering

- Clustering signature database
  - Fuzzy C Means Clustering

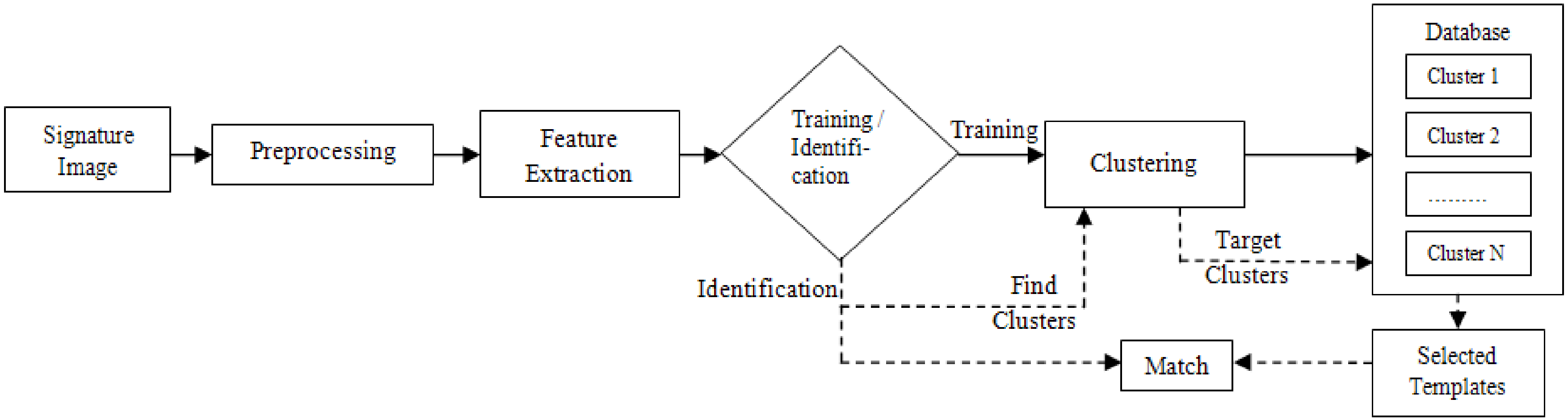

Results

Table: Bin miss rate for different clusters using FCM and K-means

No. of Clusters	FCM	K-means
2	1	0
3	2	0
4	3	1
5	8	8
6	11	12
7	12	18
8	16	21
9	17	25

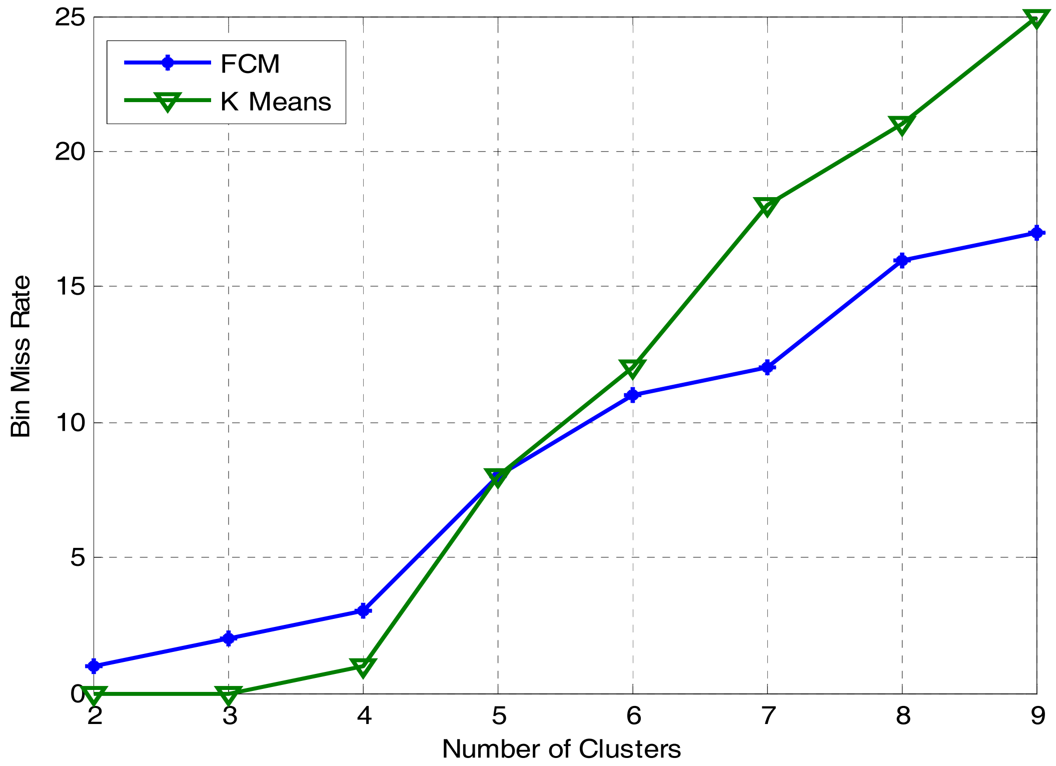

Graph showing bin miss rate by varying number of clusters for FCM and K-Means

Indexing Database

- Features are extracted using blockwise DCT
- Coefficients are reordered into subbands
- Histogram is obtained for each subband (H_i)
- A global key is obtained using histogram binning approach
- B-tree is traversed using global key

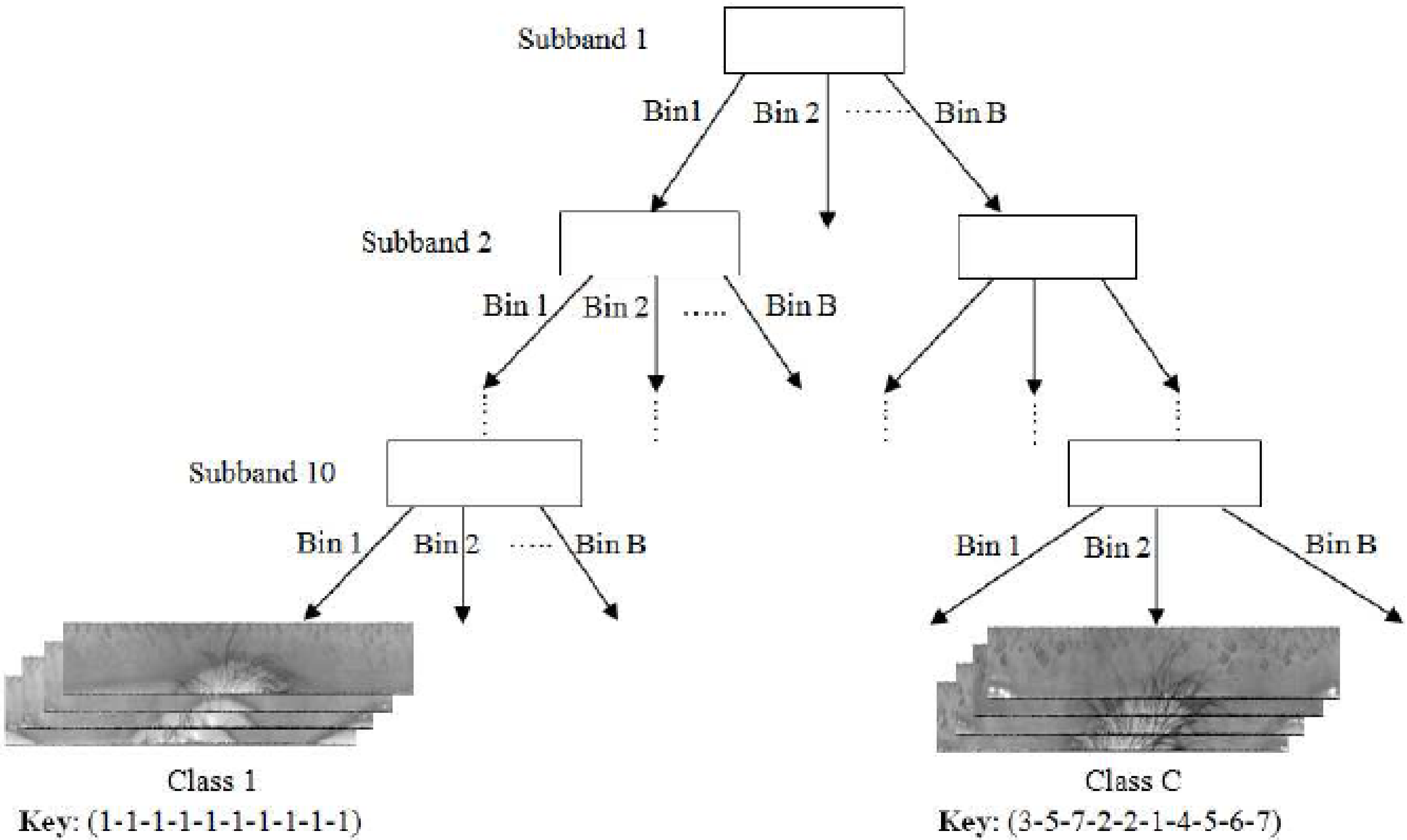
Subband 1
Bin1
Bin 2
Bin B
Subband 2
Bin 1
Bin 2
.....
Bin B
Subband 10
Bin 1
Bin 2
Bin B
Bin 1
Bin 2
Bin B
Class 1
Key: (1-1-1-1-1-1-1-1-1-1)
Class C
Key: (3-5-7-2-2-1-4-5-6-7)

System Diagram

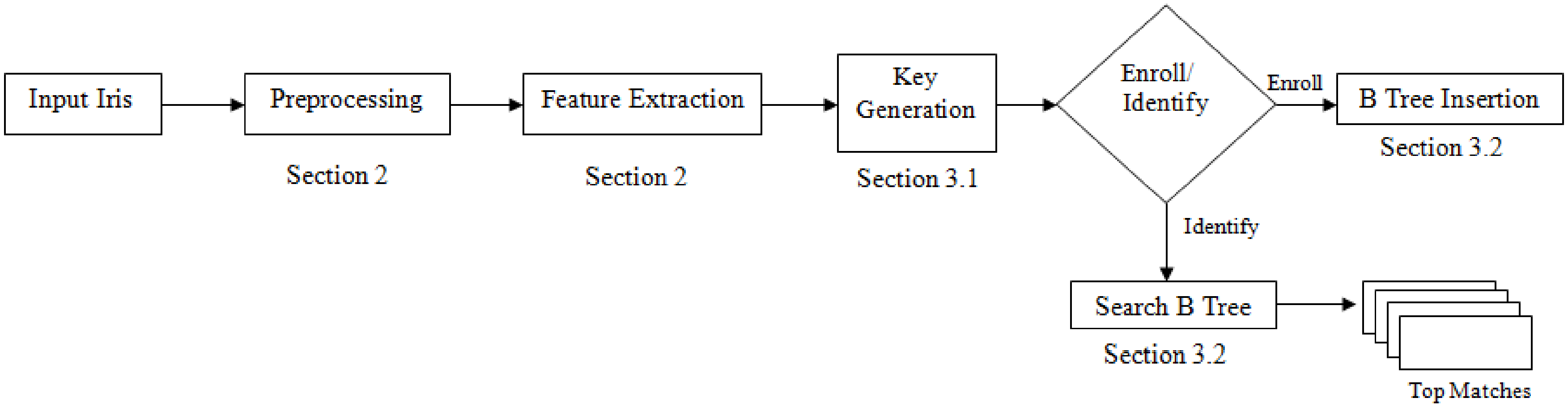

Results

Subband (#)	CASIA			BATH			IITK		
	Classes (#)	BM	PR	Classes	BM	PR	Classes	BM	PR
1	2	0.00	99.69	5	04	26.14	5	1.5	41.44
2	5	1.60	35.96	23	12	7.69	19	5.0	17.21
3	16	3.60	22.70	66	26	3.04	46	5.5	9.24
4	39	13.2	10.23	130	36	1.42	93	10.0	4.77
5	82	24.0	6.12	197	38	0.92	148	12.5	3.25
6	158	30.8	3.46	313	56	0.49	252	15.5	1.56
7	233	35.6	2.63	399	60	0.30	396	20.5	0.92
8	304	40.0	1.77	492	70	0.16	584	29.0	0.50
9	387	42.0	1.22	583	72	0.09	744	37.5	0.27
10	519	43.6	0.63	648	72	0.06	856	44.0	0.20

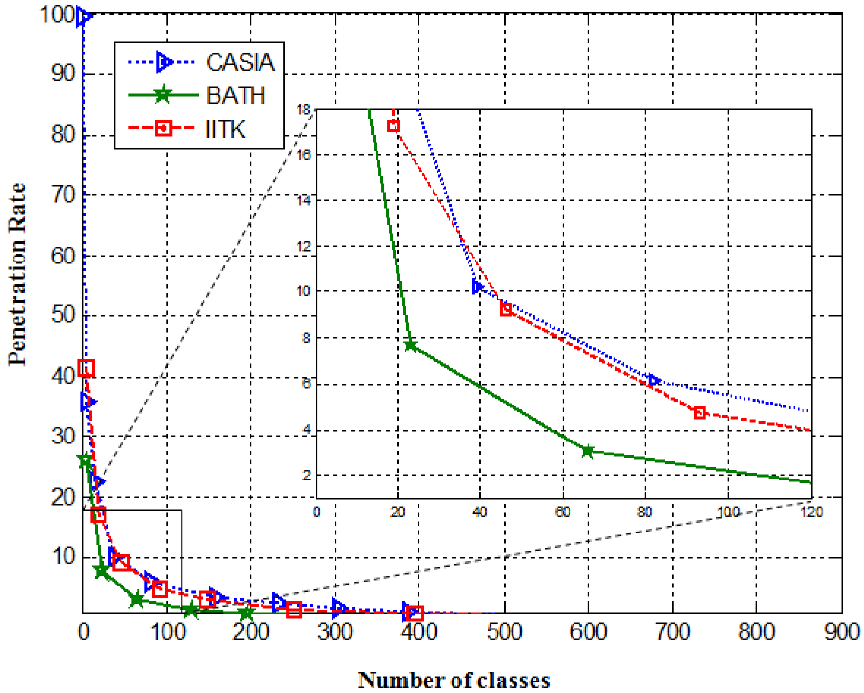
CASIA
BATH
IITK
Penetration Rate
Number of classes

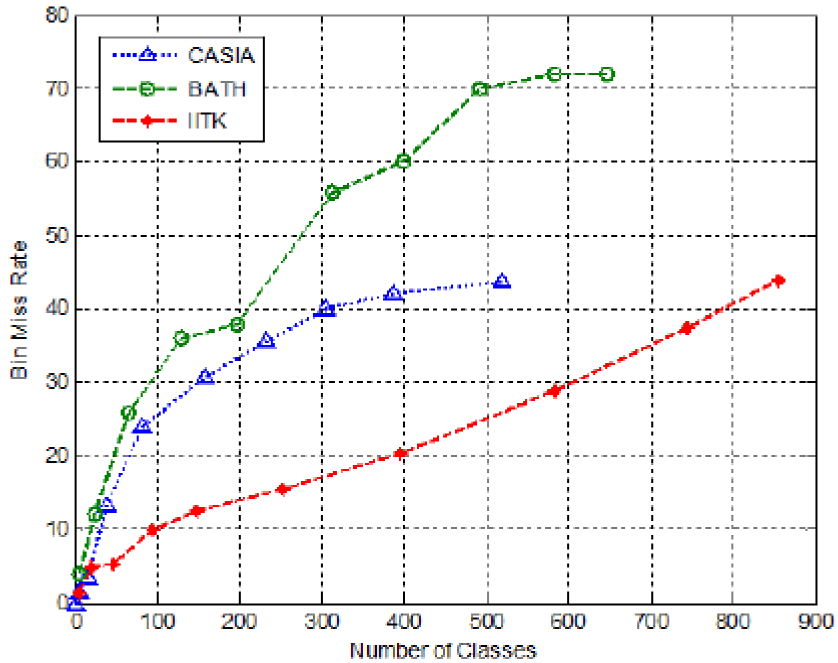
CASIA
BATH
IITK
Bin Miss Rate
Number of Classes

Local feature descriptor for Iris

- To further improve accuracy

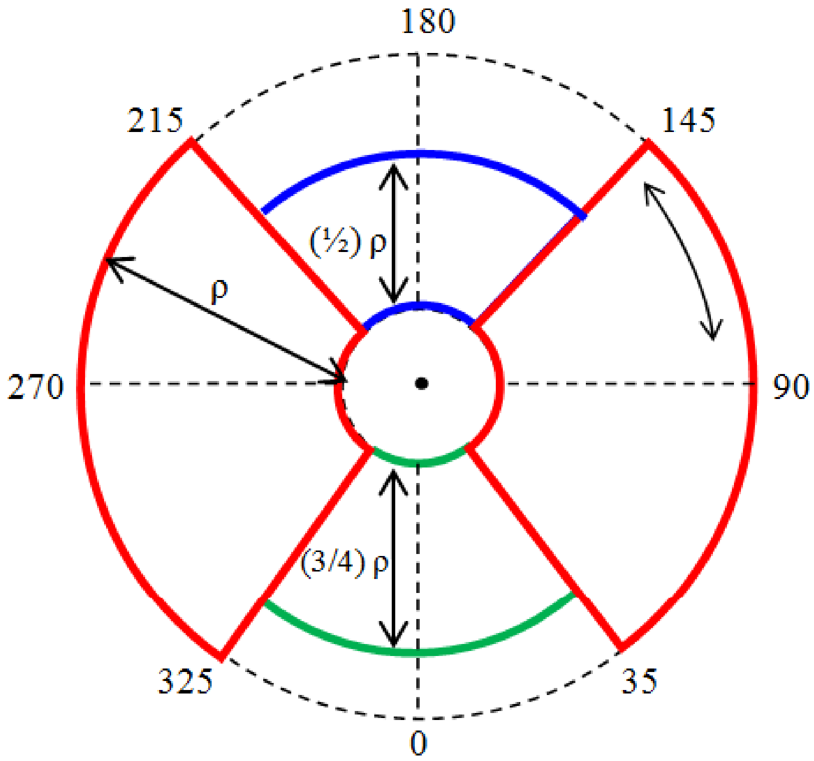

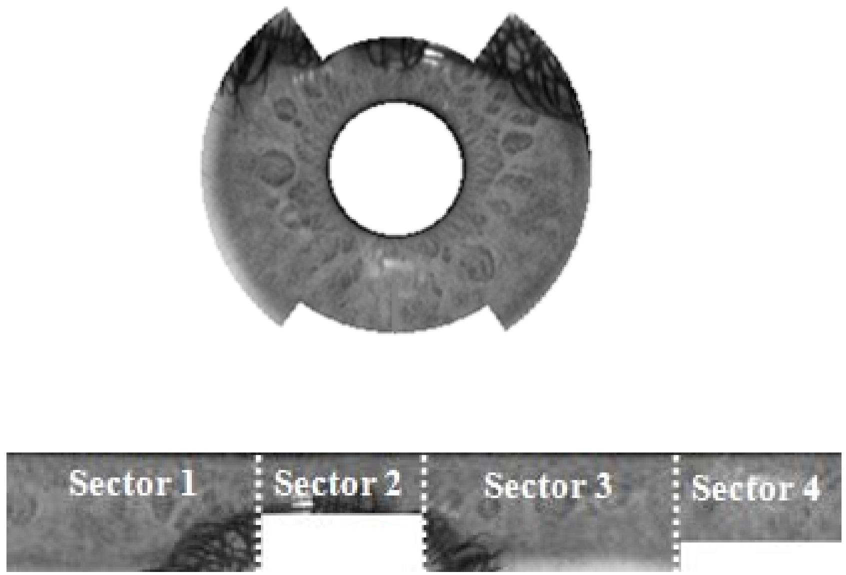

- Features are extracted using Speeded Up Robust Features
  - Uses Hessian Matrix
  - Descriptor is formed using Haar Wavelet responses

- Pairing of features using nearest neighbor approach

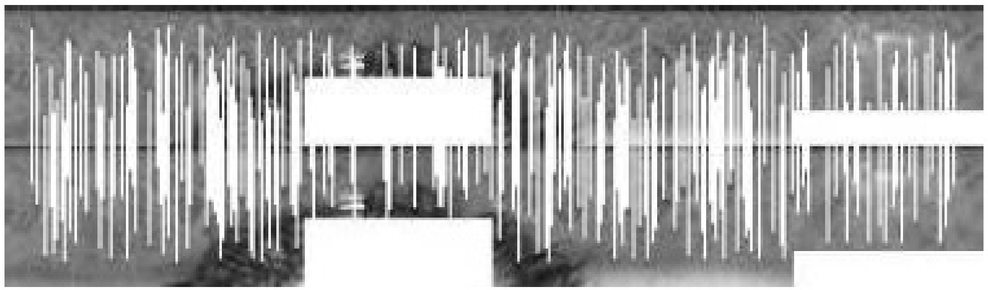

Results

- Accuracy has been increased considerably

	BATH			CASIA			IITK		
Approaches	FAR	FRR	Acc	FAR	FRR	Acc	FAR	FRR	Acc
Gabor	1.63	8.02	95.16	3.47	44.94	75.78	2.64	21.09	88.13
Harris	29.04	39.03	65.97	17.18	34.73	74.05	24.95	21.95	76.55
SIFT	0.77	16.41	91.54	15.12	28.22	78.32	1.99	31.37	83.31
SURF	2.66	6.36	95.48	4.58	3.85	95.77	0.02	0.01	99.98

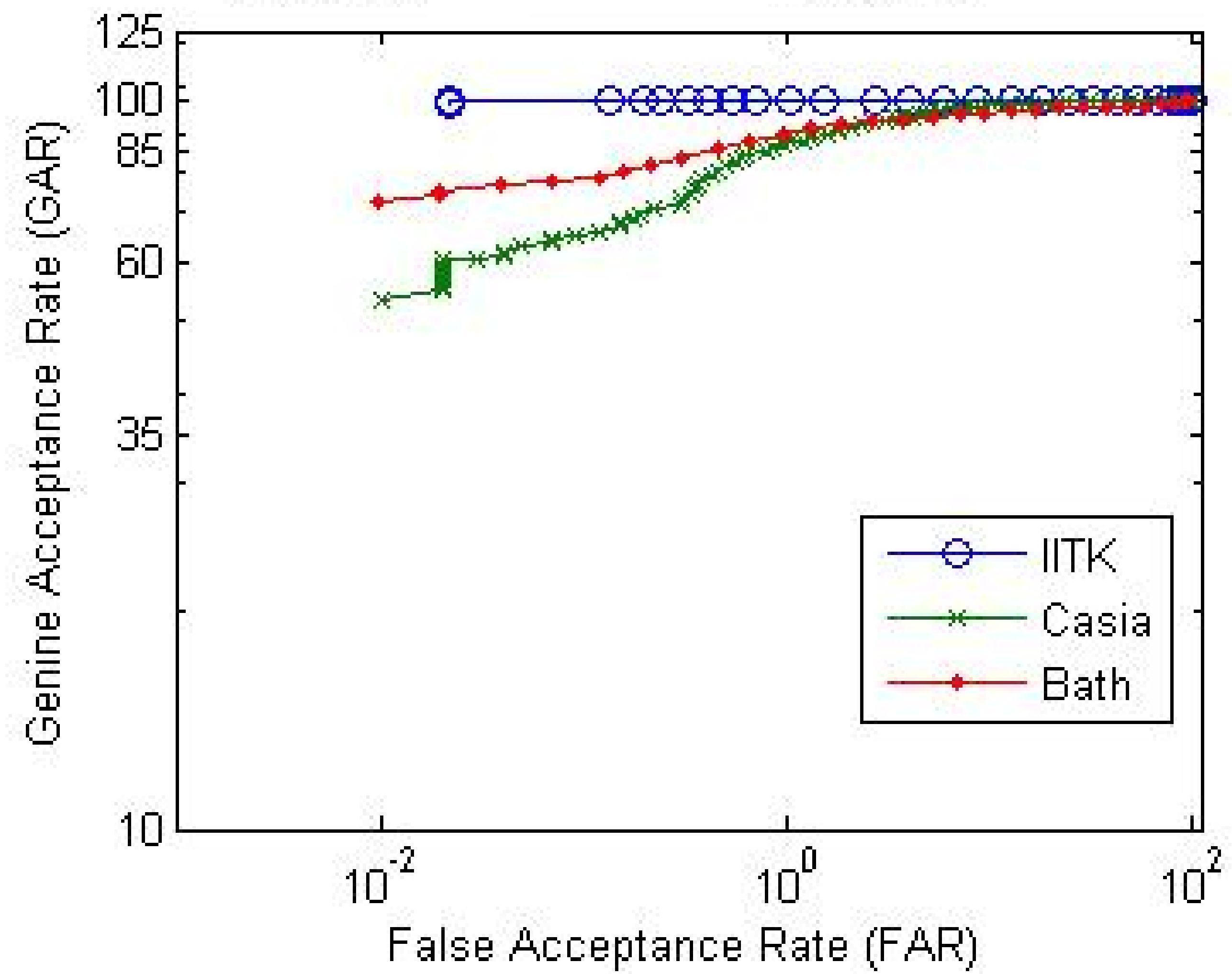
125
100
85
60
35
10
Genine Acceptance Rate (GAR)
10^{-2}
10^{0}
10^{2}
False Acceptance Rate (FAR)
IITK
Casia
Bath

Annular Iris Recognition

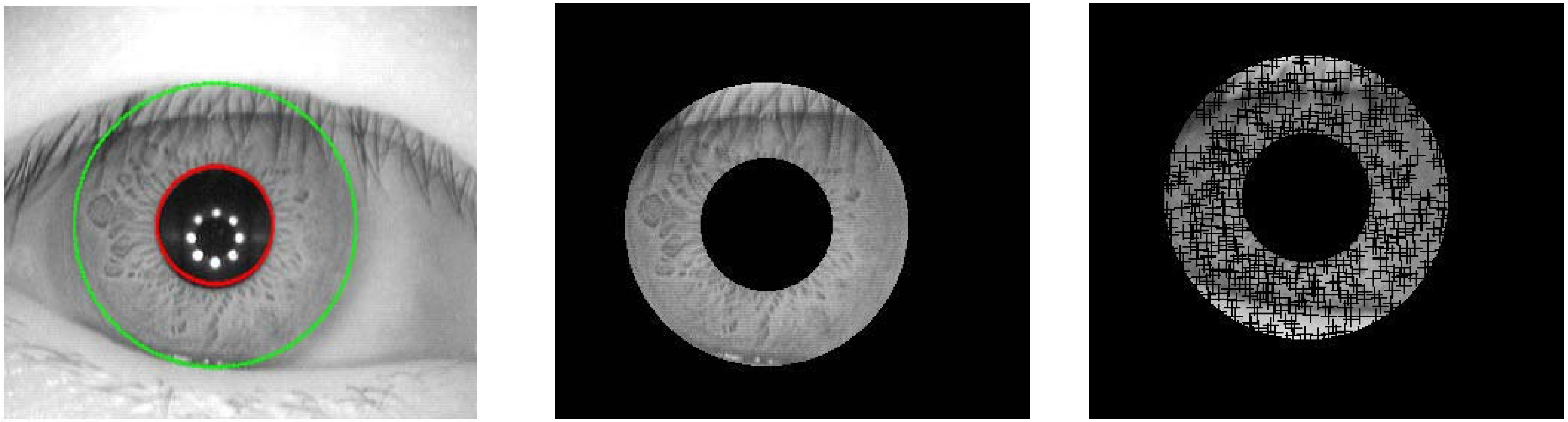

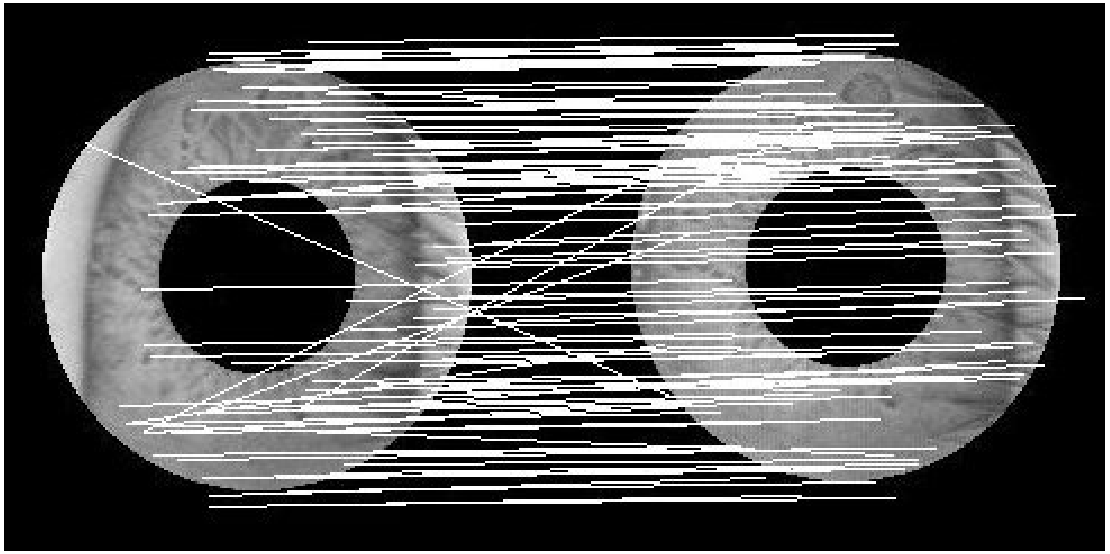

Results

Database →	BATH			CASIA			IITK		
Test cases ↓	**FAR**	**FRR**	**Acc**	**FAR**	**FRR**	**Acc**	**FAR**	**FRR**	**Acc**
Normalized Iris	10.35	21.11	84.26	3.31	5.13	95.77	0.86	5.52	98.60
Annular Iris	2.37	1.97	97.84	1.44	4.07	97.23	4.65	1.41	97.15

Results

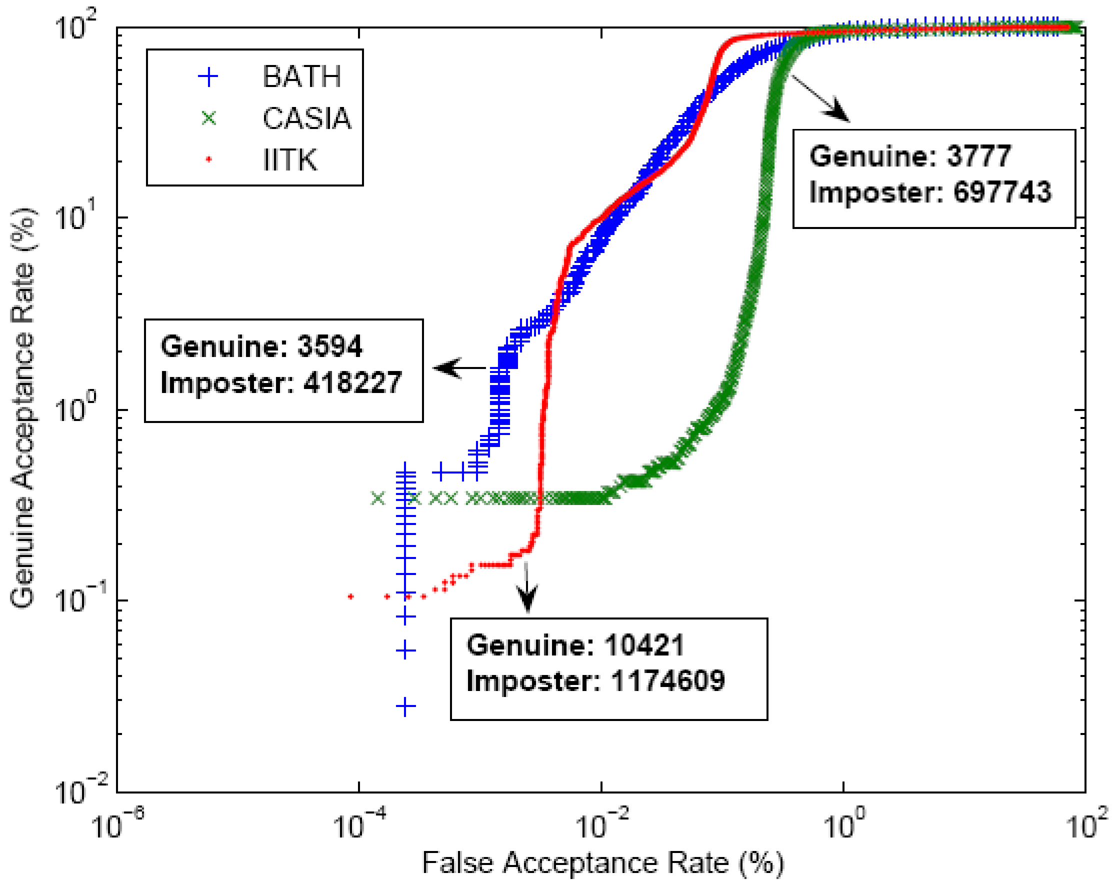

BATH
CASIA
IITK
Genuine: 3777
Imposter: 697743
Genuine: 3594
Imposter: 418227
Genuine: 10421
Imposter: 1174609
Genuine Acceptance Rate (%)
False Acceptance Rate (%)

Iris Biometric-Applications

- IBM Looks Airline Security in the Eye
- IrisGuard, Inc.
- Securimetrics, Inc.
- Panasonic
- London Heathrow Airport
- Amsterdam Schiphol Airport
- Charlotte Airport USA
- IrisAccess LG Corp, South Korea
- IrisPass OKI Electric Industries, Japan
- EyeTicket Corp. USA

Case studies on Iris

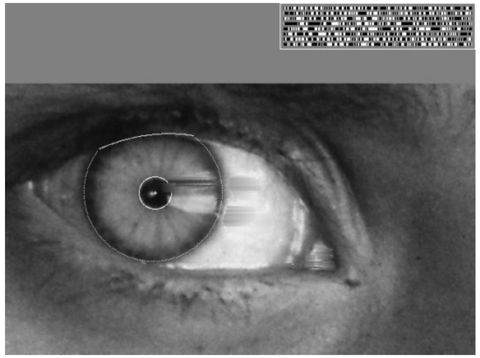

Source: http://www.cl.cam.ac.uk/~jgd1000/afghan.html

Employees at Albany International Airport (NY)

Frequent Flyers at Schiphol Airport (NL)

Frequent Flyers at Schiphol Airport (NL) may enroll in the "Privium" programme, enabling them to enter The Netherlands without passport presentation.

Condominium residents in Tokyo gain entry to the building by their iris patterns, and the elevator is automatically called and programmed to bring them to their residential floor.

United Nations High Commission for Refugees administers cash grants to refugees returning into Afghanistan

Frequent Flyers at Frankfurt/Main Airport can pass quickly through Immigration Control without passport inspection if their iris patterns have been enrolled for this purpose.

The check-in procedure for passengers at Narita Airport (Japan) is expedited by recognition of their iris patterns

References

- A. K. Jain, A. Ross, and S. Prabhakar, S., "An introduction to biometric recognition," IEEE Transactions on Circuits and Systems for Video Technology, vol.14, no.1, pp. 4-20, Jan. 2004
- A. Ross, A. K. Jain, and J. Z. Qian, "Information Fusion in Biometrics", Proc. 3rd International Conference on Audio- and Video-Based Biometric Person Authentication, pp. 354-359, Sweden, June 6-8, 2001
- Phalguni Gupta, Ajita Rattani, Hunny Mehrotra, Anil K. Kaushik, “Multimodal biometrics system for efficient human recognition”, Proc. SPIE International Society of Optical Engineering 6202, 62020Y, 2006

- L. Flom, A. Safir, Iris recognition system, U.S. Patent 4641394, 1987
- J. Daugman, How iris recognition works, Image Processing. 2002. Proceedings. 2002 International Conference on , vol.1, no., pp. I-33-I-36 vol.1, 2002
- R. P. Wildes, Iris recognition: an emerging biometric technology, Proceedings of the IEEE , vol.85, no.9, pp.1348-1363, Sep 1997
- K.W. Bowyer, K. Hollingsworth, P.J. Flynn, Image Understanding for Iris Biometrics: A Survey, Computer Vision and Image Understanding, 2007

Link for Databases

- Casia : http://www.cbsr.ia.ac.cn/IrisDatabase.htm
- Bath University: http://www.bath.ac.uk/elec-eng/research/sipg/irisweb/index.htm
- MMU: http://pesona.mmu.edu.my/~ccteo/
- UBIRIS: http://iris.di.ubi.pt/
- IITK: http://www.cse.iitk.ac.in/users/biometrics/

Thank you.